The correction vector method for three-photon absorption: The effects of π conjugation in extended rylenebis(dicarboximide)s

Yuanping Yi, Lingyun Zhu, and Zhigang Shuai

Citation: The Journal of Chemical Physics **125**, 164505 (2006); doi: 10.1063/1.2355676
View online: https://doi.org/10.1063/1.2355676
View Table of Contents: http://aip.scitation.org/toc/jcp/125/16
Published by the American Institute of Physics

The correction vector method for three-photon absorption: The effects of π conjugation in extended rylenebis(dicarboximide)s

Yuanping Yi, Lingyun Zhu, and Zhigang Shuai[a)]
Key Laboratory of Organic Solids, Beijing National Laboratory for Molecular Sciences (BNLMS), Institute of Chemistry, Chinese Academy of Sciences, 100080 Beijing, China

(Received 4 August 2006; accepted 23 August 2006; published online 24 October 2006)

A correction vector method within the multireference determinant single and double configuration interaction approximation coupled with the semiempirical intermediate neglect of differential overlap Hamiltonian has been developed for the computation of single and multiphoton absorption spectra of conjugated molecules. We study the effect of π conjugation on these properties in the extended rylenebis(dicarboximide)s. The one-, two-, and three-photon absorption cross sections of the lowest-lying excited states show a power law dependence on the conjugation length, with exponents of about 1.3, 2.6, and 5.6, respectively. The maximum value of the three-photon absorption cross section in these molecules is calculated to be 1.06×10^{-78} cm^6 s^2/photon^2 for photon energy at 0.57 eV. © *2006 American Institute of Physics*. [DOI: 10.1063/1.2355676]

I. INTRODUCTION

The study of organic conjugated molecules with efficient multiphoton absorption (MPA) properties has received considerable attention because of their potential applications in the fields of optical power limiting,[1–3] three-dimensional (3D) fluorescence imaging,[4,5] 3D microfabrication,[6] and photodynamics therapy.[7] Three-photon absorption (3PA) is a process in which a molecule absorbs three photons simultaneously. Compared to two-photon absorption (2PA), 3PA-based novel materials may exhibit two major advantages: (1) much longer IR wavelengths can be used and (2) much better beam confinement can be achieved owing to the cubic dependence of nonlinear absorption on the local intensity of the excitation IR light.[8,9]

It is well recognized that the large optical nonlinearities in conjugated systems are determined primarily by the highly delocalized π electron. It leads to low excitation energies and large transition dipole moments, translating together into high nonlinear electrical polarizabilities. Recently, Pschirer *et al.*[10] have synthesized a series of rylenebis(dicarboximide)s which displays good chemical and thermal stabilities and have remarkable photophysical properties. By extending the aromatic π system along the molecular long axis, the π-electron conjugation length is elongated.

In this paper, we investigated the 3PA properties of these molecules using correction vector (CV) approach coupled with multireference single and double configuration interaction (MRDCI) method. The CV method is equivalent to sum over states, but it needs only the ground state properties, thus avoiding the impossible tasks of solving all the excited states. It is found that by extending the π-electron conjugation length the 3PA cross section at the resonance energy is enhanced by two orders of magnitude.

[a)]Author to whom correspondence should be addressed. Electronic mail: zgshuai@iccas.ac.cn

II. THEORETICAL METHODOLOGY

The widely used theoretical method to calculate the nonlinear optical (NLO) properties is the sum-over-states (SOS) method.[11] In this method, the NLO coefficients of a molecule can be expressed as sums over transition dipole moment products with transition energies as denominators. For example, the first-order polarizability α can be expressed as

$$\alpha_{ij}(\omega)=\sum_R\left[\frac{\langle G|\tilde{\mu}_i|R\rangle\langle R|\tilde{\mu}_j|G\rangle}{E_R-E_G-\hbar\omega-i\Gamma}+\frac{\langle G|\tilde{\mu}_j|R\rangle\langle R|\tilde{\mu}_i|G\rangle}{E_R-E_G+\hbar\omega+i\Gamma}\right], \tag{1}$$

where $|G\rangle$ and $|R\rangle$ are the ground state and the excited state wave vectors of the system, and E_G and E_R are the corresponding energies, ω is the fundamental input frequency, Γ denotes Lorentzian broadening factor, $\tilde{\mu}_i$ is the dipole displacement operator,

$$\tilde{\mu}_i=\bar{\mu}_i-\langle G|\bar{\mu}_i|G\rangle, \tag{2}$$

and the indices i and j are the Cartesian coordinates. As we know, the practical application of SOS method usually involves a truncation in the summation, because it is extremely difficult to obtain all the excited state information for a medium or large size of molecule with correlated π electrons. This truncation may lead to uncontrolled errors. For multiphoton absorption, one can also use tensor approach,[12,13] which also involves SOS but with less folds of summation. This problem can be solved by employing the CV method as first suggested by Ramasesha and Soos.[14] The CV method provides results which are exactly equal to those of a sum over all states within a given configuration space. For the two-photon absorption, the CV methods have been implemented in the semiempirical CISD framework.[15] In this method one can obtain the NLO coefficients without explicitly calculating the large number of excited states of the Hamiltonian and the transition dipole moments among these states. By introducing the correction vectors, the summation

can be avoided. For the first-order polarizability α, starting from the sum-over-state expression, it can also be expressed as

$$\alpha_{ij}(\omega) = \sum_R \left[\frac{\langle G|\tilde{\mu}_i|R\rangle\langle R|\tilde{\mu}_j|G\rangle}{E_R - E_G - \hbar\omega - i\Gamma} + \frac{\langle G|\tilde{\mu}_j|R\rangle\langle R|\tilde{\mu}_i|G\rangle}{E_R - E_G + \hbar\omega + i\Gamma} \right]$$
$$= \left\langle G|\tilde{\mu}_i|\frac{1}{H - E_G - \hbar\omega - i\Gamma}|\tilde{\mu}_j|G\right\rangle + \left\langle G|\tilde{\mu}_j|\frac{1}{H - E_G - \hbar\omega - i\Gamma}|\tilde{\mu}_i|G\right\rangle$$
$$= \langle \phi_i^{(1)}(-\omega)|\tilde{\mu}_j|G\rangle + \langle \phi_j^{(1)}(\omega)|\tilde{\mu}_i|G\rangle, \quad (3)$$

where $|\phi_i^{(1)}(\omega)\rangle$ and $|\phi_i^{(1)}(-\omega)\rangle$ are defined through the following first-order correction vector equation:

$$(H - E_G + \hbar\omega_1 + i\Gamma_1)|\phi_i^{(1)}(\omega_1)\rangle = \tilde{\mu}_i|G\rangle, \quad (4)$$

$$(H - E_G + \hbar\omega_1 + i\Gamma_1)|\phi_i^{(1)}(-\omega_1)\rangle = \tilde{\mu}_i|G\rangle, \quad (5)$$

In Eq. (3), we have made use the mathematical fact that an eigenvector $|R\rangle$ of an operator H is also the eigenvector of a function of the operator $f(H)$.

Similarly, the second- and third-order correction vectors (corrections to the ground state wave vector upon frequency-dependent perturbation), $|\phi_{ij}^{(2)}(\omega_1,\omega_2)\rangle$ and $|\phi_{ijk}^{(3)}\times(\omega_1,\omega_2,\omega_3)\rangle$, can be deduced, which obey the following linear equations:

$$(H - E_G + \hbar\omega_2 + i\Gamma_2)|\phi_{ij}^{(2)}(\omega_1,\omega_2)\rangle = \tilde{\mu}_j|\phi_i^{(2)}(\omega_1)\rangle, \quad (6)$$

$$(H - E_G + \hbar\omega_3 + i\Gamma_3)|\phi_{ijk}^{(3)}(\omega_1,\omega_2,\omega_3)\rangle = \tilde{\mu}_k|\phi_{ij}^{(2)}(\omega_1,\omega_2)\rangle. \quad (7)$$

In our calculations, the absolute values of Γ_1, Γ_2, and Γ_3 are set to be 0.1 eV. Formally, $|\phi_i^{(1)}(\omega_1)\rangle$, $|\phi_{ij}^{(2)}(\omega_1,\omega_2)\rangle$, and $|\phi_{ijk}^{(3)}(\omega_1,\omega_2,\omega_3)\rangle$ can be expanded in the basis of the eigenstates of the Hamiltonian, $\{|R\rangle\}$, $\{|S\rangle\}$, and $\{|T\rangle\}$,

$$|\phi_i^{(1)}(\omega_1)\rangle = \sum_R C_R|R\rangle,$$

$$C_R = \frac{\langle R|\tilde{\mu}_i|G\rangle}{E_R - E_G + \hbar\omega_1 + i\Gamma_1}, \quad (8)$$

$$|\phi_{ij}^{(2)}(\omega_1,\omega_2)\rangle = \sum_S C_S|S\rangle,$$

$$C_S = \frac{\langle S|\tilde{\mu}_j|\phi_i^{(1)}(\omega_1)\rangle}{E_S - E_G + \hbar\omega_2 + i\Gamma_2} = \sum_R \frac{\langle S|\tilde{\mu}_j|R\rangle\langle R|\tilde{\mu}_i|G\rangle}{(E_S - E_G + \hbar\omega_2 + i\Gamma_2)(E_R - E_G + \hbar\omega_1 + i\Gamma_1)}, \quad (9)$$

$$|\phi_{ijk}^{(3)}(\omega_1,\omega_2,\omega_3)\rangle = \sum_T C_T|T\rangle,$$

$$C_T = \frac{\langle T|\tilde{\mu}_k|\phi_{ij}^{(2)}(\omega_1,\omega_2)\rangle}{E_T - E_G + \hbar\omega_3 + i\Gamma_3} = \sum_S \sum_R \frac{\langle T|\tilde{\mu}_k|S\rangle\langle S|\tilde{\mu}_j|R\rangle\langle R|\tilde{\mu}_i|G\rangle}{(E_T - E_G + \hbar\omega_3 + i\Gamma_3)(E_S - E_G + \hbar\omega_2 + i\Gamma_2)(E_R - E_G + \hbar\omega_1 + i\Gamma_1)}. \quad (10)$$

By comparing with the SOS formulation, the first-order polarizability α, the third-order polarizability γ, and the five-order polarizability ε can be written in terms of the correction vectors as

$$\alpha_{ij}(\omega_\sigma;\omega_1) = P_{ij}\langle \phi_i^{(1)}(-\omega_1)|\tilde{\mu}_j|G\rangle, \quad (11)$$

$$\gamma_{ijkl}(\omega_\sigma;\omega_1,\omega_2,\omega_3) = P_{ijkl}\langle \phi_i^{(1)}(-\omega_1-\omega_2-\omega_3)|\tilde{\mu}_j|\phi_{kl}^{(2)} \times(-\omega_1-\omega_2,-\omega_1)\rangle, \quad (12)$$

$$\varepsilon_{ijklmn}(\omega_\sigma;\omega_1,\omega_2,\omega_3,\omega_4,\omega_5) = P_{ijklmn}\langle \phi_{ij}^{(2)}(-\omega_1-\omega_2,-\omega_1)|\tilde{\mu}_k|\phi_{lmn}^{(3)} \times(-\omega_3-\omega_4-\omega_5,-\omega_3-\omega_4,-\omega_3)\rangle. \quad (13)$$

Here, $\omega_\sigma = -\omega_1-\omega_2-\omega_3-\omega_4-\omega_5$; the operators P generate all permutations: (ω_σ,i), (ω_1,j), (ω_2,k), (ω_3,l), (ω_4,m), and (ω_5,n), leading to two terms for α, 24 terms for γ, and 720 terms for ε. For one-photon absorption (1PA), $\omega_1=\omega$, for 2PA, $\omega_1=\omega_3=\omega$, $\omega_2=-\omega$, and for 3PA $\omega_1=\omega_3=\omega_4=\omega$, $\omega_2=\omega_5=-\omega$. Note that, in most linear conjugated systems, the component of the MPA amplitude along the molecular long axis is dominant to any other tensor component. So in the following, only this component is calculated explicitly. Thus the 1PA, 2PA, and 3PA cross sections (σ_1, σ_2, and σ_3) can be expressed (in cm^2, cm^4 s/photon, and cm^6 s^2/photon^2) as

$$\sigma_1 = \frac{4\pi L^2}{\hbar nc}(\hbar\omega)\,\mathrm{Im}\,\alpha_{xx}(-\omega;\omega), \quad (14)$$

$$\sigma_2 = \frac{4\pi^2 L^4}{\hbar n^2 c^2}(\hbar\omega)^2\,\mathrm{Im}\,\gamma_{xxxx}(-\omega;\omega,-\omega,\omega), \quad (15)$$

$$\sigma_3 = \frac{4\pi^3 L^6}{3\hbar n^3 c^3}(\hbar\omega)^3\,\mathrm{Im}\,\varepsilon_{xxxxxx}(-\omega;\omega,-\omega,\omega,-\omega,\omega), \quad (16)$$

where c is the speed of light in vacuum, n is a refractive index (set to 1.0 in vacuum), and $L=(n^2+2)/3$ denotes a

local field correction. It is found that for the multiphoton absorption, the contributions of resonant terms are dominant. There are 4 and 36 resonant terms for 2PA and 3PA among all 24 and 720 terms, respectively.[13] Thus σ_2 and σ_3, when averaged over molecular orientations assuming an isotropic sample (assuming linearly polarized light) can be written as[13,16]

$$\sigma_2 = \frac{4}{5}\frac{4\pi^2 L^4}{\hbar n^2 c^2}(\hbar\omega)^2 \,\mathrm{Im}\langle \phi_x^{(1)}(-\omega)|\tilde{\mu}_x|\phi_{xx}^{(2)}(-2\omega,-\omega)\rangle, \tag{17}$$

$$\sigma_3 = \frac{364\pi^3 L^6}{73\hbar n^3 c^3}(\hbar\omega)^3 \,\mathrm{Im}\langle \phi_{xx}^{(2)}(-2\omega,-\omega)|\tilde{\mu}_x|\phi_{xxx}^{(3)} \times(-3\omega,-2\omega,-\omega)\rangle. \tag{18}$$

The Hamiltonian matrix dimension is usually tremendously large. In general, it is impossible to diagonalize the whole matrix to obtain all the excited states. However, for the linear equations, Eqs. (4)–(7), only one vector is needed to resolve, much as getting one eigenvector, which is certainly much easier numerically than to get all the eigenvectors.

It is necessary to find an effective approach to solve the linear equations (4)–(7) to get a satisfactory 1PA, 2PA, or 3PA spectrum. We use a small matrix algorithm[17] parallel to Davidson's diagonalization algorithm for solving these equations for both positive and negative ω.[14] In this algorithm, with a set of orthonormalized vectors Q, the large system $Ax=b$ is transformed to a small one $Q^T AQy=Q^T b$ which can be solved directly with the LAPACK program package.[18] The solution of the large system is obtained by the sum of the transforming vectors Q_i multiplied by the coefficients y_i, $x=\Sigma_{i=1}^{n} y_i Q_i$. Then the residue vector R_n, which is the difference between the left-hand side and the right-hand side of the large system, is calculated. If the desired convergence is not achieved, the Q space is augmented by adding a new vector Q_{n+1}, which is the normalized projection of S_n perpendicular to all old transforming vectors. The vector S_n is given by $S_{n,i}=R_{n,i}/A_{ii}$. Then the iterative process is continued. When the size of small matrix exceeds a defined number N (set to 50), the whole process is restarted with one transforming vector $Q_1=x$. The initial Q_1 is given by $Q_{1,l}=b_i/A_{il}$. For nonpositive definite matrix A (for instance, for negative ω), the linear equation is transformed to $A^T Ax=A^T b$. Then the small matrix formulation is changed to be $Q^T A^T AQy=Q^T A^T b$. The rest procedures are the same as before. That is to say, the initial Q vector is given by $Q_{1,i}=b_i/A_{ii}$, the residue vector R_n equals $Ax-b$, the vector S_n is given by $S_{n,i}=R_{n,i}/A_{ii}$, and the added Q vector is obtained by the same way. If no component of the residue vector R_n is greater than 10^{-6}, the iterative process is converged.

III. COMPUTATIONAL DETAILS

The chemical structures of the molecules studied in the present work are displayed in Fig. 1. The molecules in experiment[10] are slightly different from those in our calculations. Namely, the alkyl or aryl and tert-octylphenoxy groups

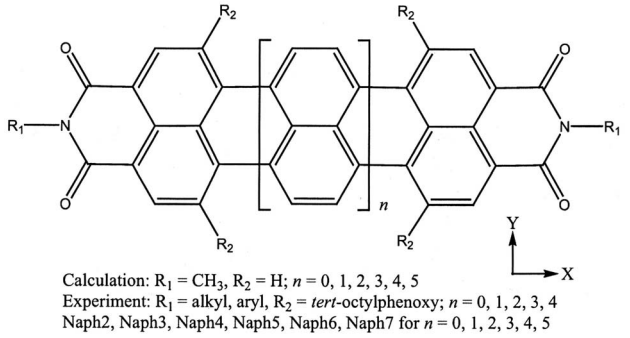

FIG. 1. Chemical structures of the extended rylenebis(dicarboximide)s. The *XYZ* reference frame is also shown.

are replaced by methyl and hydrogen groups, respectively, for simplicity of computations. The ground state geometries of the molecules are optimized at the density-functional theory (DFT) level with the hybrid Beck three-parameter Lee-Yang-Parr (B3LYP) functionals and the 6-31G basis set, as implemented in the GAUSSIAN 03 package.[19]

From the optimized geometries, we constructed the multireference single and double configuration interaction[20] coupled to the semiempirical intermediate neglect of differential overlap (INDO) Hamiltonian[21] (MRDCI/INDO) and the transition dipole moment matrix. It is shown that the MRDCI/INDO is necessary for calculating the higher-order NLO properties of conjugated system. The Mataga-Nishimoto potential[22] is used to describe the Coulomb repulsion terms. By diagonalizing the Hamiltonian for the lowest-lying state (not for many high-lying excited states), we obtain the ground-state energy and its corresponding wave function. In the MRDCI calculations, we only take π orbitals into consideration.[23] For molecules Naph2 and Naph3 the active space includes all continuous highest occupied π orbitals and all continuous lowest unoccupied π orbitals. 11 occupied molecular orbitals and 11 unoccupied molecular orbitals are included for other molecules. To construct the configuration space, we choose six important reference configurations including the Hartree-Fock ground state, three single-excitation configurations [highest occupied molecular orbital (HOMO) → lowest unoccupied molecular orbital (LUMO), HOMO−1 → LUMO, and HOMO → LUMO+1], and two double-excitation configurations (HOMO, HOMO → LUMO, LUMO and HOMO−1, HOMO → LUMO, LUMO+1), amounting to about 220 000 configurations in total. We note that in the standard ZINDO calculations, only 2 occupied and 2 unoccupied MOs have been taken in such calculations for the 2PA properties and only about 200 configurations in total are taken in the CI calculations, namely many important molecular orbitals as well as configuration contributions have been vastly ignored.[24] A previous extended version of ZINDO program has been successfully applied to calculate the nonlinear optical properties and multiphoton absorptions, which allowed up to 6000 configurations of six occupied–six unoccupied active MO space.[25] The present approach has vastly exceeded these limits, which allows us to investigate larger molecules. We note that in DALTON program package,[26] the nonlinear response theory[27] has

TABLE I. Optimized ground state geometries of the calculated molecules.

Molecule	Top view	Side view
Naph2	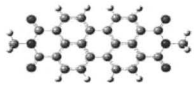	
Naph3	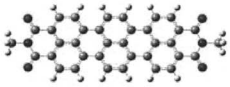	
Naph4	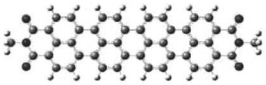	
Naph5	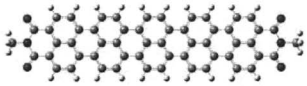	
Naph6		
Naph7		

been implemented to evaluate the MPA cross section. Indeed, Luo and co-workers have extensively applied this approach to design molecules with interesting MPA properties.[28] However, we note that it is very difficult to obtain a dynamic MPA spectrum from their method: the convergence is not guaranteed when the input frequency or its multiples approach or exceed the lowest excited state energy. In principle, our approach is equivalent to the nonlinear response approach. Since our method is always definite positive for the linear algebra equation, the iteration is always converged for any input frequency. To the best of our knowledge, this work represents the first nonlinear response function method for the full electronic spectroscopy, containing the resonance features in the MPA spectra.

IV. RESULTS AND DISCUSSION

A. Molecular geometries and electronic structure

The optimized ground-state geometries of the molecules are displayed in Table I. The molecules are the fully planar and centrosymmetric conjugated systems, which easily lead to a highly delocalized π-electron cloud. In Table II, we present the conjugation length, lowest two excited state excitation energy, and the transition moments obtained by our MRDCI/INDO, the conjugation length of the molecules being taken as the distance between nitrogen atoms at both ends of the chain.

For centrosymmetric systems, one of the most important features is that the 2PA active state and the ground state are of the same symmetry, but the symmetry of 1PA or 3PA active state is the inverse symmetry of the ground state. We find that for Naph7, the first singlet excited state (S1) is a 2PA active state, the second singlet excited state (S2) is a 1PA or 3PA active state, but the inverse case is for the other molecules. As a result of the symmetry, the transition dipole moment between the ground state and the 2PA active state is

TABLE II. The molecular conjugation length (L), the excitation energies (E_{01} and E_{02}) of the first two singlet excited states (S1 and S2), and the x component of the transition dipole moments (M_{01} and M_{02}) between the excited states and the ground state.

Molecule	Naph2	Naph3	Naph4	Naph5	Naph6	Naph7
L (Å)	11.42	15.76	20.09	24.43	28.76	33.10
E_{01} (eV)	2.89	2.47	2.19	2.02	1.82	1.69
E_{02} (eV)	3.43	2.68	2.35	2.12	1.84	1.69
M_{01} (D)	9.47	12.56	15.56	18.26	21.65	0.00
M_{02} (D)	0.00	0.00	0.00	0.00	0.00	24.37

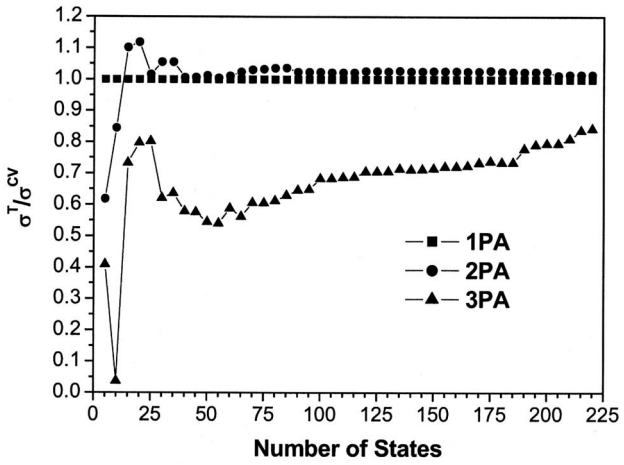

FIG. 2. Evolution of the 1PA, 2PA, and 3PA cross sections obtained by the tensor approach at the first peak of Naph2 as a function of the number of the excited states involved in the summation. The square, circle, and triangle dot lines correspond to 1PA, 2PA, and 3PA, respectively.

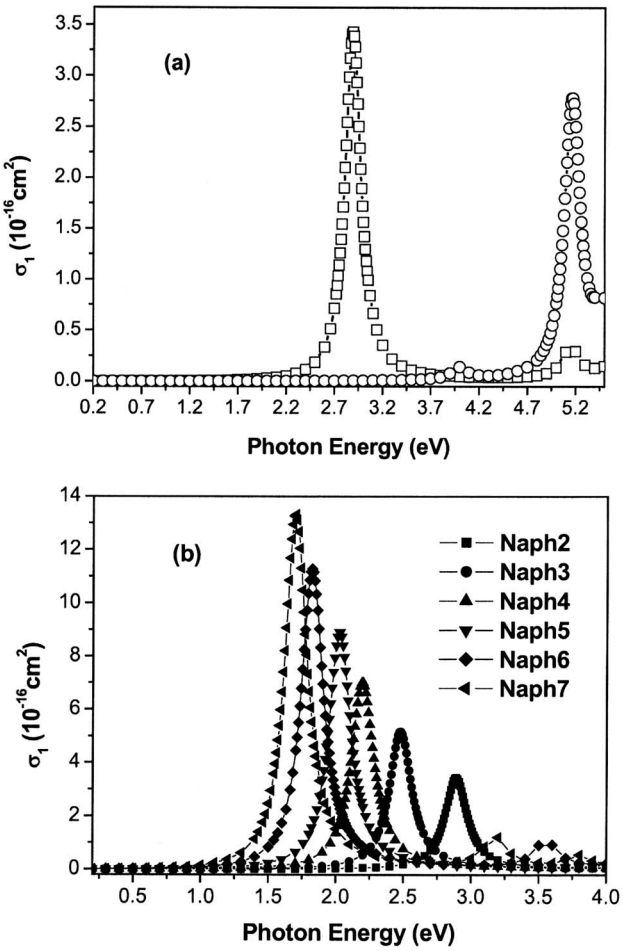

FIG. 3. One-photon absorption spectrum: (a) MRDCI-polarized linear absorption spectrum of Naph2. The open square and open circle dot lines correspond to polarization along the *X* and *Y* axes, respectively. (b) The *x*-polarized linear absorption spectrum of the calculated molecules: Naph2 (square), Naph3 (circle), Naph4 (upper triangle), Naph5 (lower triangle), Naph6 (diamond), and Naph7 (left triangle).

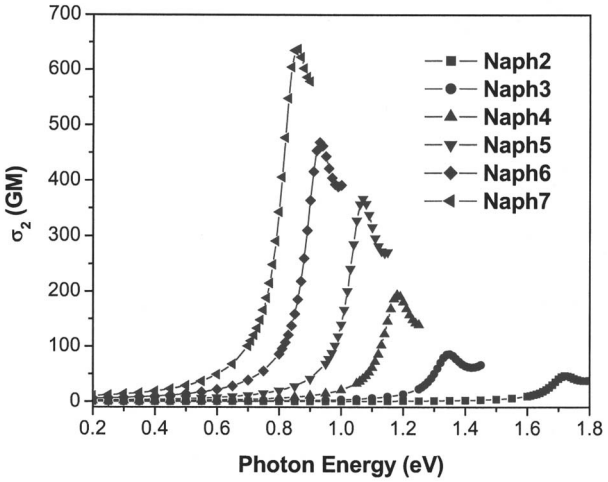

FIG. 4. The calculated two-photon absorption spectra of Naph2 (square), Naph3 (circle), Naph4 (upper triangle), Naph5 (lower triangle), Naph6 (diamond), and Naph7 (left triangle). (1 GM=10^{-50} cm^4 s/photon).

zero. We note that, by extending the conjugation length, the excitation energies decrease and the difference between S1 and S2 becomes smaller and that the transition dipole moment between the ground state and the first 1PA active state increases with the number of inserted naphthalene groups.

B. Convergence test

Before discussing the multiphoton absorption properties of the studied molecules, we investigated the evolution of σ_1, σ_2, and σ_3 of Naph2 obtained by the tensor approach with the number of the involved states at the photon energy of the first peak. From Fig. 2, we find that the σ_1 obtained by the tensor approach with a few states is virtually identical with that by the CV method. However, σ_2 is underestimated by ca. 38% including only five excited states in the summation, while the inclusion of 20 excited states will lead to σ_2 being overestimated by ca. 12%. σ_2 will not converge well until including about 200 excited states. For σ_3, it is not converged all the time and is underestimated by ca. 16% even if as many as 220 excited states are included. In one word, to obtain the converged values, more and more excited states must be required for increasing numbers of absorbed photons. Here, the advantage of CV method is clearly manifested that it gives directly the converged MPA spectra based only on the ground state knowledge.

C. One-photon absorption

Figure 3(a) displays the MRDCI/INDO polarized absorption spectrum of Naph2. In the spectral range with lower photon energy, the linear spectrum is characterized by the *x*-polarized (the direction connecting two N–N atoms, the reference framework is also shown in Fig. 1) feature at ca. 2.9 eV. The *y*-polarized absorption peak at ca. 5.2 eV is dominant in high-energy region. The experimental linear absorption spectrum[10] of Naph2 is dominated by two features

TABLE III. The 1PA, 2PA, and 3PA photon energies at the first peak and the corresponding cross sections (σ_1, σ_2, and σ_3).

Molecule	1PA peak (eV)	2PA peak (eV)	3PA peak (eV)	σ_1 (10^{-16} cm^2)	σ_2 (GM)	σ_3 (10^{-80} cm^6 s^2/photon^2)
Naph2	2.89	1.72	0.97	3.43	47.0	0.26
Naph3	2.48	1.35	0.83	5.16	86.0	2.27
Naph4	2.20	1.18	0.74	7.01	193.4	7.56
Naph5	2.02	1.07	0.68	8.91	366.8	24.59
Naph6	1.82	0.93	0.61	11.27	468.4	51.05
Naph7	1.70	0.86	0.57	13.31	637.8	106.46

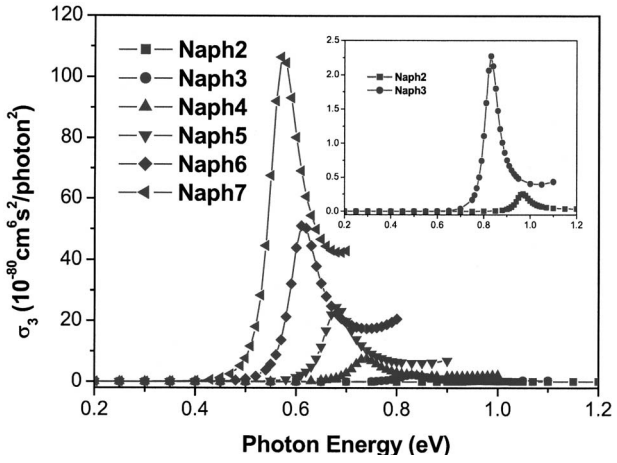

FIG. 5. The calculated three-photon absorption spectra of Naph2 (square), Naph3 (circle), Naph4 (upper triangle), Naph5 (lower triangle), Naph6 (diamond), and Naph7 (left triangle). The spectra of Naph2 and Naph3 are enlarged in the inset for the sake of clarity of presentation.

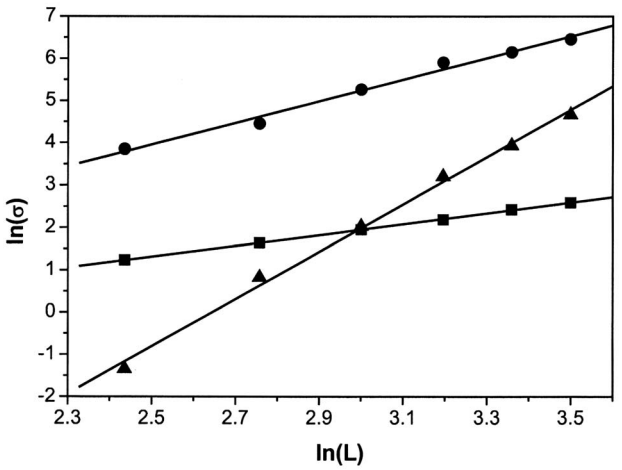

FIG. 6. The log-log plot of cross section vs the molecule length [$\ln(\sigma_1)$, $\ln(\sigma_2)$, $\ln(\sigma_3)$ vs $\ln(L)$, where σ value is taken at the first peak]. The square, circle, and triangle dot lines correspond to 1PA, 2PA, and 3PA, respectively.

at 2.1 and 4.3 eV, respectively. In our investigation into MPA we concentrate on the spectral range of low photon energy for its potential application, therefore the *y*-polarized effect plays a minor role in the MPA response and will not be discussed further. The calculated *x*-polarized absorption spectrum of all molecules is shown in Fig. 3(b). We note that the overall shape of the spectrum compares very well to the experimental spectrum in the range of low photon energy. The increase of the conjugation length by adding extra naphthalene groups enhances the 1PA peak intensity and makes the peak redshifted. It is expected that a similar change should be observed for the 3PA due to the same transition rules for 1PA and 3PA.

D. Two-photon absorption

The simulated 2PA spectra of the studied molecules are shown in Fig. 4. We find that the 2PA cross section is sizable and the spectrum is dominated by a single peak associated with a singlet excited state (S2 for Naph2 to Naph6 and S1 for Naph7). With the increase of the conjugation length, such as going from Naph2 to Naph7, the 2PA peak is redshifted and the σ_2 of Naph7 is enhanced by ca. 13 times compared with Naph2, amounting to 637.8 GM at 0.86 eV (see Table III).

E. Three-photon absorption

Figure 5 shows the calculated frequency-dependent 3PA spectra of the six molecules in a spectral range for which the molecules are transparent for both 1PA and 2PA. As in the case of 2PA, the 3PA spectra in the calculated region are characterized by the presence of a single strong resonance related to the lowest 1PA active state (S1 for Naph2 to Naph6, S2 for Npah7). As expected, with the increase of the conjugation length from Naph2 to Naph7, the 3PA peak is redshifted and the corresponding σ_3 is enhanced. For instance, the σ_3 of Naph7 is about two orders of magnitude larger than that of Naph2, amounting to 1.06×10^{-78} cm^6 s^2/photon^2 and the photon energy at the peak is reduced by 0.4 eV (see Table III). A power law dependence on the π-electron conjugation lengths of σ_1, σ_2, and σ_3 is presented in Fig. 6 for all calculated molecules. The simulated exponents are 1.3, 2.6, and 5.6 for 1PA, 2PA, and 3PA, respectively. The much larger power of increase for σ_3 compared with σ_2 and σ_1 can be induced by the higher orders of transition dipole moment products and detuned transition energy denominators.

V. CONCLUSIONS

To summarize, we have successfully implemented the correction vector method for the computation of dynamic single and multiphoton absorption spectra of π-conjugated systems within the multireference determinants with single and double configuration interaction approximation coupled with the semiempirical intermediate neglect of differential overlap Hamiltonian. It is shown that the ground-state-based CV method is exactly equivalent to the SOS method but avoids the difficulty to resolve excited states. From our calculations, it is shown that within the SOS approach, even when considering a few hundred excited states, the result is still far from the converged value for 3PA. The effect of the π-electron conjugation length on the one-, two-, and three-photon absorption properties in extended rylenebis(dicarboximide)s is investigated. The one-, two-, and three-photon absorption cross sections of the lowest-lying excited states show a power law dependence on the conjugation length, with exponents of about 1.3, 2.6, and 5.6, respectively. The maximum value of the three-photon absorption cross section in these molecules is calculated to be 1.06×10^{-78} cm^6 s^2/photon^2 for photon energy at 0.57 eV.

ACKNOWLEDGMENTS

This work is supported by NSFC (Grant Nos. 10425420, 20433070, and 20421101) as well as the CNIC supercomputer center of the Chinese Academy of Sciences.

[1] J. S. Shirk, R. G. S. Pong, F. J. Bartoli, and A. W. Snow, Appl. Phys. Lett. **63**, 1880 (1993).
[2] J. W. Perry, K. Mansour, S. R. Marder, K. J. Perry, D. Alvarez, Jr., and I. Choong, Opt. Lett. **19**, 625 (1994).
[3] J. W. Perry, K. Mansour, I.-Y. S. Lee *et al.*, Science **273**, 1533 (1996).
[4] W. Denk, J. H. Strickler, and W. W. Webb, Science **248**, 73 (1990).
[5] P. T. C. So, C. Y. Dong, B. R. Masters, and K. M. Berland, Annu. Rev. Biomed. Eng. **2**, 399 (2000).
[6] B. H. Cumpston, S. P. Ananthavel, S. Barlow *et al.*, Nature (London) **398**, 51 (1999).
[7] W. G. Fisher, W. P. Partridge, C. Dees, and E. A. Wachter, Photochem. Photobiol. **66**, 141 (1997).
[8] G. S. He, J. D. Bhawalkar, and P. N. Prasad, Opt. Lett. **20**, 1524 (1995).
[9] G. S. He, P. P. Markowicz, T. C. Lin, and P. N. Prasad, Nature (London) **415**, 767 (2002).
[10] N. G. Pschirer, C. Kohl, F. Nolde, J. Qu, and K. Müllen, Angew. Chem., Int. Ed. **45**, 1401 (2006).
[11] B. J. Orr and J. F. Ward, Mol. Phys. **20**, 513 (1971).
[12] P. Cronstrand, Y. Luo, P. Norman, and H. Ågren, Chem. Phys. Lett. **375**, 233 (2003).
[13] L. Zhu, X. Yang, Y. Yi, P. Xuan, Z. Shuai, D. Chen, E. Zojer, J. L. Brédas, and D. Beljonne, J. Chem. Phys. **121**, 11060 (2004); L. Zhu, Y. Yi, Z. Shuai, J. L. Brédas, D. Beljonne, and E. Zojer, *ibid.* **125**, 044101 (2006).
[14] S. Ramasesha and Z. G. Soos, Chem. Phys. Lett. **153**, 171 (1988); Z. Shuai, S. Ramasesha, and J. L. Brédas, *ibid.* **250**, 14 (1996); S. Ramasesha, Z. Shuai, and J. L. Brédas, *ibid.* **245**, 224 (1995); S. K. Pati, S. Ramasesha, Z. Shuai, and J. L. Brédas, Phys. Rev. B **59**, 14827 (1999).
[15] P. C. Ray and J. Leszczynski, J. Phys. Chem. A **109**, 6689 (2005); P. C. Jha, M. Das, and S. Ramasesha, *ibid.* **108**, 6279 (2004).
[16] W. M. McClain, J. Chem. Phys. **55**, 2789 (1971); **57**, 2264 (1972); P. Norman, P. Cronstrand, and J. Ericsson, Chem. Phys. Lett. **285**, 207 (2002).
[17] S. Ramasesha, J. Comput. Chem. **11**, 545 (1990).
[18] E. Anderson, Z. Bai, C. Bischof *et al.*, LAPACK *Users Guide*, Third Edition, Society for Industrial and Applied Mathematics, Philadelphia, PA, 1999; Available from http://www.netlib.org/lapack/
[19] M. J. Frisch, G. W. Trucks, H. B. Schlegel *et al.*, GAUSSIAN 03, Gaussian Inc., Carnegie, PA, 2003.
[20] R. J. Buenker and S. D. Peyerimhoff, Theor. Chim. Acta **35**, 33 (1974); P. Tavan and K. Schulten, J. Chem. Phys. **85**, 6602 (1986); Z. Shuai, D. Beljonne, and J. L. Brédas, *ibid.* **97**, 1132 (1992).
[21] J. Ridley and M. C. Zerner, Theor. Chim. Acta **32**, 111 (1973).
[22] N. Mataga and K. Z. Nishimoto, Phys. Chem. **12**, 35 (1957); **13**, 140 (1957).
[23] I. D. L. Albert, J. O. Morley, and D. Pugh, J. Chem. Phys. **102**, 237 (1995).
[24] X. Zhou, A. Ren, J. Feng, and X. Liu, J. Phys. Chem. A **107**, 1850 (2003); Chem. Phys. Lett. **373**, 167 (2003).
[25] E. Zojer, D. Beljonne, T. Kogej, H. Vogel, S. R. Marder, J. W. Perry, and J. L. Brédas, J. Chem. Phys. **116**, 3646 (2002); D. Beljonne, W. Wenseleers, E. Zojer, Z. Shuai, H. Vogel, S. J. K. Pond, J. W. Perry, S. R. Marder, and J. L. Brédas, Adv. Funct. Mater. **12**, 631 (2002); E. Zojer, W. Wenseleers, P. Pacher, S. Barlow, M. Halik, C. Grasso, J. W. Perry, S. R. Marder, and J. L. Brédas, J. Phys. Chem. B **108**, 8641 (2004).
[26] T. Helgaker, H. J. Aa. Jensen, P. Jørgensen *et al.*, DALTON, an *ab initio* electronic structure program, 2001 Release 1.2; available from http://www.kjemi.uio.no/software/dalton/dalton.html
[27] J. Olsen and P. Jørgensen, J. Chem. Phys. **82**, 3235 (1985).
[28] P. Cronstrand, Y. Luo, and H. Ågren, Adv. Quantum Chem. **50**, 1 (2005); P. Cronstrand, P. Norman, Y. Luo, and H. Ågren, J. Chem. Phys. **121**, 2020 (2004); P. Cronstrand, B. Jansik, D. Jonsson, Y. Luo, and H. Ågren, *ibid.* **121**, 9239 (2004).